Special AT-rich sequence-binding protein 2 suppresses invadopodia formation in HCT116 cells via palladin inhibition

Mohammed A. Mansour[1], Eri Asano[1], Toshinori Hyodo[1], KA Akter[1], Masahide Takahashi[2], Michinari Hamaguchi[1], Takeshi Senga[1]

[1]Division of Cancer Biology, [2]Department of Pathology, Nagoya University Graduate School of Medicine, 65 Tsurumai, Showa, Nagoya, 466-8550 Japan

Address correspondence to:

Mohammed Mansour; 65 Tsurumai, Showa, Nagoya, 466-8550, Japan

Phone: 81-52-744-2463; Fax: 81-52-744-2464; E-mail: biomansour@hotmail.com

Takeshi Senga M.D., Ph.D.; 65 Tsurumai, Showa, Nagoya, 466-8550, Japan

Phone: 81-52-744-2463; Fax: 81-52-744-2464; E-mail: tsenga@med.nagoya-u.ac.jp

Running title: SATB2 inhibits palladin in CRC

Keywords: Colorectal Cancer; SATB2; Invadopodia; palladin

Abstract

Invadopodia are specialized actin-based microdomains of the plasma membrane that combine adhesive properties with matrix degrading activities. Proper functioning of the bone, immune, and vascular systems depend on these organelles, and their relevance in cancer cells is linked to tumor metastasis. The elucidation of the mechanisms driving invadopodia formation is a prerequisite to understanding their role and ultimately to controlling their functions. Special AT-rich sequence-binding protein 2 (SATB2) was reported to suppress tumor cell migration and metastasis. However, the mechanism of action of SATB2 is unknown. Here, we show that SATB2 inhibits invadopodia formation in HCT116 cells and that the molecular scaffold palladin is inhibited by exogenous expression of SATB2. To confirm this association, we elucidated the function of palladin in HCT116 using a knock down strategy. Palladin knock down reduced cell migration and invasion and inhibited invadopodia formation. This phenotype was confirmed by a rescue experiment. We then demonstrated that palladin expression in SATB2-expressing cells restored invadopodia formation. Our results showed that SATB2 action is mediated by palladin inhibition and the SATB2/palladin pathway is associated with invadopodia formation in colorectal cancer cells.

1. Introduction

Colorectal cancer (CRC) is the second leading cause of cancer deaths, with approximately 500,000 deaths per year worldwide. Over the past two decades, several treatments have been identified for CRC patients. However, the rate of recurrence and failure after these treatments remains high. Additionally, most CRC deaths are associated with tumor invasion and metastasis (1). Thus, there is a strong impetus to understand the function of cancer genes involved in CRC invasiveness to develop new therapeutic approaches.

Special AT-rich sequence-binding protein 2 (SATB2) is a member of the SATB family proteins, which share structural homology consisting of CUT and homeobox domains (2). SATB2 is a transcriptional factor that specifically binds to the nuclear matrix attachment region (MAR) of AT-rich DNA sequences to regulate chromatin remodeling and transcription (3,4). SATB2 has multiple roles in developmental processes including craniofacial patterning, brain development, and osteoblast differentiation (5). The chromosomal deletions of 2q33.1 that cause SATB2 haploinsufficiency in humans are associated with a cleft or high palate, facial dysmorphism, and intellectual disability (6,7). In addition to critical roles for developmental processes, previous studies have demonstrated that SATB2 is associated with tumor suppression. An immunohistochemical analysis of laryngeal squamous cell carcinoma (LSCC) showed that lower expression of SATB2 was correlated with advanced clinical staging, histological grade and tumor recurrence (8). In colorectal cancer, high expression of SATB2 is associated with good prognosis and sensitivity to chemotherapy and radiation (9,10). These studies indicate that high expression of SATB2 is a promising marker for the good prognosis of cancer patients; however, detailed analysis of SATB2 function in cancer cells has not been fully performed.

Palladin (PALLD) is an actin-associated protein with multiple isoforms derived from a single gene (11). A recent review by L. Jin (12) described 7 isoforms and the Universal Protein Database currently shows 9 isoforms of human palladin. Palladin is widely expressed in various tissues and cell lines as major 90 and 140 kDa isoforms, whereas 200 kDa palladin is specifically detected in heart and bone (11). Palladin has an essential role in the assembly and maintenance of multiple types of actin-rich structures, including stress fibers, dynamic dorsal ruffles and matrix-degrading podosomes (13,14). Accumulating evidence has revealed that palladin is associated with malignant characteristics of cancer. Goicoechea et al. (15) reported that palladin was localized to the invadopodia of cancer cells and played important roles for invasion of metastatic breast cancer cells. In pancreatic cancer, palladin is

expressed in cancer associated fibroblast (CAF) and an animal model demonstrated that palladin expression in CAF enhanced invasion of pancreatic cancer cells (16,17). In addition, a recent study showed that palladin interacts with membrane-type 1 matrix metalloproteinase (MMP14) to promote degradation of the extracellular matrix (ECM). This interaction links ECM degradation to cytoskeletal dynamics and migration signaling in mesenchymal breast cancer cells (18). These studies clearly indicate that palladin plays an important role for the promotion of cancer cell invasion.

In this study, we demonstrate that exogenous expression of SATB2 inhibits invadopodia formation and invasion of colorectal cancer cells. SATB2 expression suppressed expression of palladin, and restoration of palladin expression rescued SATB2-mediated inhibition of invasion and invadopodia formation. This study define a novel SATB2/palladin pathway for the suppression of tumor invasion.

2. Materials and methods

Cells and antibodies

HCT116, CW-2 and COLO 320 cells were obtained from ATCC and cultured in DMEM (HCT116) and RPMI (CW-2 & COLO 320), supplemented with 10% FBS and antibiotics. HEK293T cells used for retrovirus production were maintained in DMEM with 10% FBS. The antibodies were obtained from the following companies: anti-ß-actin, Sigma-Aldrich (St. Louis, MO); anti-SATB2, Abcam (Cambridge, UK); anti-GFP, Neuro Mab (Davis, CA); anti-α-tubulin, Sigma-Aldrich (St. Louis, MO). Anti-palladin antibody was generated previously (19).

Generation of stable cell lines

Full-length SATB2 and palladin (90 kDa form) were PCR amplified from a cDNA library of HCT116 cells. SATB2 was cloned into the pQCXIP vector with an N-terminal GFP tag or FLAG tag and transfected into 293T cells together with the pVPack-GP and pVPack-Ampho vectors using Lipofectamine 2000 (Invitrogen, Carlsbad, CA). Forty-eight hours after transfection, the supernatants were added to cells with 2 µg/ml polybrene (Sigma-Aldrich). The infected cells were selected by incubating with 1 µg/ml puromycin for 2 days.

To establish HCT116 cell lines that constitutively expressed GFP, GFP-palladin (wt) (GFP-tagged wild-type palladin) and GFP-PALLD (Res) (GFP-tagged mutant palladin) each cDNA was cloned into a pQCXIN retrovirus vector (Clontech, Mountain View, CA). Silent mutations were introduced in GFP-PALLD (Res) to confer resistance to shRNA targeting endogenous palladin. Each plasmid was

transfected into HEK 293T cells together with pVPack-GP and pVPack-Ampho vectors using Lipofectamine 2000 according to the manufacturer's protocol. The culture supernatants were collected 48 h after transfection and applied to HCT116 cells in combination with 2 μg/ml polybrene (Sigma). The cells were cultured for 24 h and infected cells were selected with 400 μg/ml of G418 (Nacalai Tesque, Tokyo, Japan). To establish shLuc (Ctrl), shPALLD #1, shPALLD #2/GFP and shPALLD #2/GFP-PALLD (Res) cells, oligonucleotides encoding shRNAs specific for human palladin (#1: 5′-GTACTGGACGGCTAATGGT-3′ & #2: 5′-GCACAAAGGATGCTGTTAT-3′) and luciferase (5′-CTTACGCTGAGTACTTCGA-3′) were cloned into the pSIREN-RetroQ retroviral vector (Clontech). The cells were infected with recombinant retroviruses that encoded each shRNA and were selected with 1 μg/ml puromycin.

Quantitative reverse transcription–polymerase chain reaction

RNA was extracted from HCT116 cells using the RNeasy Mini Kit (Qiagen, Venlo, Netherlands), and cDNA was generated using PrimeScript Reverse Transcriptase (TAKARA, Tokyo, Japan). PCR was performed using the SYBR Premix Ex TaqTM II (TAKARA), and a Thermal Cycler DiceTM Real Time System TP800 (TAKARA) was used for the analysis. The relative mRNA expression levels were normalized to GAPDH. The sequences of primers used to amplify each gene were 5'-AGGTGGAGGAGTGGGTGTCGCTGTT-3' and 5'-CCGGGAAACTGTGGCGTGATGG-3' (GAPDH) and 5'-GCAATTCAATGCTGCTGAGA-3' and 5'-GTGGCTCCTTAGTGGGTGAA-3' (palladin).

Western blotting

Cell lysates were loaded on SDS-polyacrylamide gels for electrophoresis and transferred to polyvinylidene difluoride membranes (Millipore). The membranes were blocked with 1% skim milk for 1 h and then incubated with primary antibodies for 1 h. The membranes were then washed with TBS-T for 15 min and incubated with HRP-labeled secondary antibodies. The signals were detected with the ECL system (GE Healthcare BioSciences). The signal intensities were measured using Light Capture II equipped with CS analyzer (ATTO Corp., Tokyo, Japan).

Gelatin degradation

Coverslips were coated with 50 μg/ml (H_2O) Poly-L(D)-Lysine (Sigma-Aldrich), fixed with 0.5% glutaraldehyde (Sigma-Aldrich) and coated with 0.25 mg/ml fluorescein

isothiocyanate (FITC) conjugated gelatin (Elastin Products Co.). Cells were seeded on the coverslips and after 22 h, the cells were fixed and immunostained.

Wound-healing assay

Wound-healing assays were performed by scratching confluent monolayers of cells with a pipette tip and incubating the cells at 37°C with 5% CO2. The distance of the leading edge of the monolayer traveled was measured in five randomly selected fields every 12 hours. Three independent experiments were performed, and the data are shown as the mean ± SE.

Migration assay

To measure cell migration using Boyden chambers, a filter (8-µm pore size, 6.5-mm membrane diameter) was pre-coated with fibronectin over night, and 2 x 10_5 cells were seeded onto the upper surface of the chamber with DMEM and 0.1% BSA (serum-free). The lower chamber was filled with DMEM and 10% FBS (chemo-attractant). Eighteen hours after seeding, the cells were fixed with 70% methanol and stained with 0.5% crystal violet. The cells that migrated through the lower surface of the filters were counted in five randomly selected fields. Three independent experiments were performed, and the data are shown as the mean ± SE.

Invasion assay

To measure cell invasion using Boyden chambers, a filter (8-µm pore size, 6.5-mm membrane diameter) was pre-coated with matrigel (mixture of matrix molecules including laminin, collagen type IV and entactin) overnight, and 2 x 10_5 cells were seeded onto the upper surface of the chamber with DMEM and 0.1% BSA (serum-free). The lower chamber was filled with DMEM and 10% FBS (chemo-attractant). Twenty-four hours after seeding, the cells were fixed with 70% methanol and stained with 0.5% crystal violet. The cells that invaded the lower surface of the filters were counted in five randomly selected fields. Three independent experiments were performed, and the data are shown as the mean ± SE.

Immunofluorescence microscopy

Cells were grown on glass coverslips, fixed with 4% paraformaldehyde for 20 min and then permeabilized with 0.5% Triton X-100 for 3 min. The cells were blocked with phosphate-buffered saline (PBS) containing 7% fetal bovine serum for 30 min. The cells were incubated with primary antibody in PBS for 1 h and washed three times with PBS. After washing, the cells were incubated with FITC-conjugated anti-rabbit

antibody (Invitrogen) or Rhodamine-conjugated anti-mouse antibody (Invitrogen). The images were acquired using a laser scanning confocal microscope FV1000 (OLYMPUS, Tokyo, Japan). To visualize the actin cytoskeleton the fixed cells were incubated with rhodamine-conjugated phalloidin for 30 min and washed.

Statistical analysis

The statistical analysis is indicated in each corresponding figure legend. All data are the mean ± SE from 3 independent assays. All analyses were examined using the SigmaPlot program version 10.0 (Systat Software, Inc., San Jose, CA). The P- values were calculated from two-tailed statistical tests. A difference was considered statistically significant when $P < 0.05$.

3. Results

3.1. SATB2 expression inhibits invadopodia formation

SATB2 has been shown to have tumor suppression function and downregulation of SATB2 is associated with metastasis and poor prognosis in CRC. We generated HCT116 cells that constitutively expressed FLAG-SATB2 or FLAG tag and examined cell invasion. Expression of FLAG-SATB2 was significantly higher than endogenous SATB2 (Fig. 1A). We assessed cell invasion using a matrigel-coated Boyden Chamber. As shown in Fig. 1B, invasion of FLAG-SATB2-expressing HCT116 cells was clearly reduced compared to that of FLAG-expressing cells. Invadopodia are highly motile membrane extensions that promote degradation of extracellular matrix for cell invasion. We examined whether SATB2 expression in HCT116 cells suppressed invadopodia formation. Invadopodia are usually visualized by co-staining cells with cortactin and F-actin. Additionally, it is important to determine that the co-staining is on the ventral surface of the cell using either confocal or TIRF microscopy. We used the confocal microscopy after co-staining with phalloidin (red) and cortactin (green) to detect invadopodia. As shown in Figure 1C, the invadopodia can be identified by their dot-like concentrations of cortactin. The invadopodia were found scattered over the ventral membrane of the FLAG-expressing cells. However, FLAG-SATB2-expressing cells showed reduced dot-like concentrations of cartactin and a decreased percentage of cells with invadopodia with a 1.6-fold decrease compared to FLAG-expressing cells (Figure 1A). To confirm that the cortactin-positive dots are functional invadopodia, we used glass coverslip coated with FITC-labeled gelatin. Cells were cultured on the FITC-labeled gelatin and then degradation of gelatin was observed by confocal microscopy. Degradation of FITC-labeled gelatin was observed

where cortactin was prominently concentrated, suggesting that cortactin-rich area have ability to degrade extracellular matrix.

3.2. Expression of SATB2 inhibits palladin

Palladin was reported to promote formation of podosomes and invadopodia in normal and cancer cells, respectively (20). To elucidate the molecular mechanism by which SATB2 exerts its action, we examined palladin expression in SATB2-expressing cells. We generated either GFP- or GFP-SATB2-expressing HCT116 cells by retrovirus infection (Fig. 2A) and examined palladin mRNA level by RT-PCR. As shown in Fig. 2B, palladin mRNA was significantly reduced by GFP-SATB2 expression. To further confirm the suppression of palladin expression by exogenous SATB2, we generated CW-2 and COLO320 cells that constitutively expressed GFP-SATB2. Immunoblot analysis showed that expression of multiple palladin isoforms (200, 140, 115, 90 and 50 kDa) was significantly decreased by GFP-SATB2 (Fig. 2C).

3.3. Palladin depletion in HCT116 suppresses cell migration and invasion

We speculated that SATB2-mediated suppression of invasion and invadopodia formation were mediated by decreased palladin expression. To evaluate the function of palladin, we used two different shRNAs to deplete palladin expression. Palladin was highly expressed in HCT116, CW-2 and COLO320 cells, but not in DLD-1, CACO-2 SW620 and COLO205 cells (Fig. 3A). We used HCT116 cells for further experiment and established HCT116 cells that constitutively expressed control shRNA (shCtrl) or palladin shRNA (shPALLD#1 and shPALLD#2). Expression of palladin was clearly suppressed in shPALLD#1 and shPALLD#2 cells (Fig. 3B). We first examined cell migration in the absence of palladin. Confluent monolayers of cells were scratched and distance of the migrated leading edges was measured every 12 h. The migration of palladin-depleted cells was clearly delayed compared with that of the shCtrl cells (Fig. 3C). To further confirm this result, we used a modified Boyden chamber assay. The migration of both shPALLD#1 and shPALLD#2 cells was clearly suppressed compared with that of the shCtrl cells (Fig. 3D). We next examined cell invasion using matrigel-coated Boyden chambers. As shown in Fig. 3E, cell invasion was significantly suppressed by palladin knockdown.

3.4. Palladin localizes to invadopodia and enhances its formation

Cancer cell invasion involves degradation of ECM via formation of invasive morphological features including invadopodia. We immunostained cells for F-actin and cortactin, and then observed using a confocal microscopy to evaluate invadopodia

formation. In shCtrl HCT116 cells, invadopodia appeared as isolated puncta located behind the leading edge of the cell or under the nucleus (Figure 4A). Consistent with the reduced cell invasion in the absence of palladin, invadopodia formation was suppressed in both shPALLD#1 and shPALLD#2 cells. Nearly 60 % of shCtrl cells had cortactin concentrated area, whereas less than 30 % of palladin-depleted cells showed cortactin accumulation (Fig. 4B). These results suggest that palladin plays an important role in promoting invadopodia formation in HCT116 cells. We used immunostaining to visualize endogenous palladin in HCT116 cells to determine whether palladin is recruited to these actin-based structures. As shown in Fig. 4C, partial co-localization of palladin and cortactin was observed in HCT116 cells.

We next performed a rescue experiment using HCT116 cells to exclude the possibility that the observed phenotype was induced by the off-target effect of the shRNAs. To exogenously express palladin, we used 90 kDa isoform because the isoform is highly expressed in multiple tumor tissues and in known to promote tumor cell invasion. We generated HCT116 cells that constitutively expressed GFP or GFP-palladin(Res) by retrovirus infection. GFP-palladin(Res) has silent mutations to be resistant to shPALLD#2-mediated knockdown. Both cell lines were then infected with shPALLD #2-encoding retrovirus to generate shPALLD#2/GFP and shPALLD#2/GFP-palladin cells. Expression of endogenous palladin was reduced by shPALLD#2, but the expression of GFP-palladin(Res) was not affect (Fig. 5A). We performed an immunofluorescence analysis to observe invadopodia formation. The GFP-expressing cells showed a reduced frequency of invadopodia formation by shPALLD#2 expression. In contrast, the introduction of shPALLD#2 did not affect invadopodia formation in GFP-palladin(Res) cells (Figure 5B). These results show that invadopodia formation was specifically promoted by palladin.

3.4. SATB2 represses cell invasion and invadopodia formation via palladin inhibition

We next tested if SATB2-mediated suppression of cell invasion and invadopodia formation were mediated by palladin inhibition. We infected FLAG-SATB2 HCT116 cells with GFP or GFP-palladin (90 kDa isoform) and then assessed invadopodia formation. Although expression of endogenous palladin in FLAG-SATB2/GFP-palladin cells was reduced compared to that in FLAG cells, GFP-palladin was expressed to the level compatible with the endogenous palladin in FLAG cells (Fig. 6A). Cell invasion assay demonstrated that expression of palladin in FLAG-SATB2 cells clearly restored invasive activity similar to the level of FLAG cells (Fig. 6B). We

next examined whether invadopodia formation was restored by palladin expression. Cells were immunostained for cortactin and observed under the confocal microscopy. As shown in Figure 6B, FLAG-SATB2/GFP cells showed GFP fluorescence distributed over the cells and low dot-like concentrations of cortactin. However, FLAG-SATB2/GFP-palladin cells showed an accumulation of GFP-palladin and cortactin at the edge of cells (Fig. 6C). We quantified these results and found that the percentage of cells with invadopodia in FLAG-SATB2/GFP-palladin cells increased 1.6-fold compared to FLAG-SABT2/GFP cells. Collectively, these results indicate that the suppression of cell invasion and invadopodia formation by SATB2 was partly mediated by inhibition of palladin.

4. Discussion

In this report, we showed that SATB2 mediated inhibition of invadopodia formation and invasion was partly mediated by suppression of palladin expression. Expression of SATB2 in HCT116, CW-2, COLO320 clearly suppressed expression of multiple isoforms of palladin. In addition, palladin mRNA in HCT116 was reduced by SATB2 expression. These results clearly indicate that SATB2 expression can directly or indirectly suppress palladin expression. SATB2 has homeodomain and CUT domain that can associate with NAR or conserved DNA sequence. Analysis with deletion constructs showed that CUT domain, but not homeodomain, was critical for the suppression of palladin expression. This result indicates that CUT domain mediated SATB2 localization to NAR is critical for the palladin inhibition. SATB2-mediated chromosome rearrangement may induce structural changes in the genomic region of palladin and suppress its expression. MicroRNAs are small RNAs that bind to mRNA to inhibit translation or promote mRNA degradation. Most of the microRNA target regions are located to the 3'UTR of mRNAs. SATB2 expression suppressed multiple isoforms and they have the same 3'UTR regions. Therefore, we cannot exclude the possibility that microRNAs induced by SATB2 may have caused reduction of palladin expression.

Accumulating evidence has demonstrated that palladin plays a crucial role for cancer cell migration and invasion. Palladin can bind to multiple actin-associated proteins, such as actinin, lasp1 and CLP36, and contribute rearrangement of actin cytoskeleton for cell migration. Two opposing functions of palladin for cell migration have been reported. We and Chin et el previously reported that palladin inhibition promoted cell migration, and phosphorylation palldin by ERK or AKT regulated palladin-mediated migration suppression. In contrast, other groups clearly showed

that palldin depletion suppressed cell migration as well as actin cytoskeletal organization. In this analysis, we examined effect of palladin knockdown on cell migration using wound healing assay and transwell chamber. In both analyses, we found that palladin knockdown clearly suppressed cell migration. Organization of actin cytoskeleton is significantly different between cancer cell lines. For example, some cancer cell lines, such as SAOS2, have thick and bundled actin stress fibers, whereas many of cancer cells do not show clear formation of stress fibers. In addition, critical regulators for actin cytoskeleton and cell migration, such as RhoA, Rac1 and CDC42, show different activity among cancer cells. Depending on the cellular context, expression of palladin may promote or suppress cell migration.

In this study, we used 90 kDa form of palladin for rescue experiment. Palladin has multiple forms and most of them have C-terminal IgG domains. IgG domains are 90kDa form has three IgG domains in the C-terminus, and 140 kDa and 200 kDa have additional two IgG domains in the N-terminus. Furthermore, 140kDa and 200kDa isoforms have two SH3 binding regions, whereas 90 kDa isoform has only one region. Although a difference in function between palladin isoforms remains obscure, a previous study reported that 140 kDa has specific binding partner. Lasp1, which is an actin-binding protein, interact with proline rich region specific to 140 and 200 kDa isoforms. Overexpression of 90 kDa pallain induced bundling of stress fibers, whereas 140 kDa isoform produced star-like arrays of actin fibers, indicating these isoforms have different functions in actin cytoskeletal rearrangement. In this study, we used 90 kDa isoform for the rescue experiment. Although HCT116 cells expressed multiple isoforms of palladin and both shRNAs suppressed these isoform, expression of 90 kDa palladin was sufficient to rescue invadopodia formation and invasion. Although other isoforms may be associated with actin cytoskeletal rearrangement and cellular functions, our results show that 90 kDa palladin is a major isoform that control invadopodia formation and cell invasion.

In summary, we have shown that SATB2 expression suppressed invadopodia formation as well as invasion by inhibiting expression of palladin. Accumulating studies have shown that palladin interacts with multiple proteins and functions as a scaffold for numerous signal transductions. SATB2 may modulate signal pathways mediated by palladin for the various changes in cellular context for the suppression of tumor progression.

Acknowledgements

We would like to thank the members of the Division of Cancer Biology for their helpful discussions and Dr. Yoshihiko Yamakita (Nagoya University, Japan) for gelatin degradation assay. This research was funded by a grant from the Ministry of Education, Culture, Sports, Science and Technology of Japan (23107010 to T. Senga).

Disclosure

The authors have no conflicts of interest.

References

1. Weitz J, Koch M, Debus J, Höhler T, Galle PR, Büchler MW. Colorectal cancer. Lancet. 2005;365(9454):153-65.
2. Dobreva G, Dambacher J, Grosschedl R. SUMO modification of a novel MAR-binding protein, SATB2, modulates immunoglobulin mu gene expression. Genes Dev. 2003;17(24):3048-61.
3. FitzPatrick DR, Carr IM, McLaren L, Leek JP, Wightman P, Williamson K, et al. Identification of SATB2 as the cleft palate gene on 2q32-q33. Human molecular genetics. 2003;12(19):2491-501.
4. Britanova O, Akopov S, Lukyanov S, Gruss P, Tarabykin V. Novel transcription factor Satb2 interacts with matrix attachment region DNA elements in a tissue-specific manner and demonstrates cell-type-dependent expression in the developing mouse CNS. The European journal of neuroscience. 2005;21(3):658-68.
5. Dobreva G, Chahrour M, Dautzenberg M, et al. SATB2 is a multifunctional determinant of craniofacial patterning and osteoblast differentiation. Cell. 2006;125(5):971-86.
6. Britanova O, Depew MJ, Schwark M, et al. Satb2 haploinsufficiency phenocopies 2q32-q33 deletions, whereas loss suggests a fundamental role in the coordination of jaw development. Am J Hum Genet. 2006;79(4):668-78.
7. Rosenfeld JA, Ballif BC, Lucas A, et al. Small deletions of SATB2 cause some of the clinical features of the 2q33.1 microdeletion syndrome. PLoS ONE. 2009;4(8):e6568.
8. Liu TR, Xu LH, Yang AK, Zhong Q, Song M, Li MZ, et al. Decreased expression of SATB2: a novel independent prognostic marker of worse outcome in laryngeal carcinoma patients. PloS one. 2012;7(7):e40704.
9. Wang S, Zhou J, Wang XY, Hao JM, Chen JZ, Zhang XM, et al. Down-regulated expression of SATB2 is associated with metastasis and poor prognosis in colorectal cancer. The Journal of pathology. 2009;219(1):114-22.

10. Eberhard J, Gaber A, Wangefjord S, Nodin B, Uhlen M, Ericson Lindquist K, et al. A cohort study of the prognostic and treatment predictive value of SATB2 expression in colorectal cancer. British journal of cancer. 2012;106(5):931-8.
11. Rachlin AS, Otey CA. Identification of palladin isoforms and characterization of an isoform-specific interaction between Lasp-1 and palladin. J Cell Sci. 2006;119(Pt 6):995-1004.
12. Jin L. The actin associated protein palladin in smooth muscle and in the development of diseases of the cardiovasculature and in cancer. J Muscle Res Cell Motil. 2011;32(1):7-17.
13. Parast MM, Otey CA. Characterization of palladin, a novel protein localized to stress fibers and cell adhesions. J Cell Biol. 2000;150(3):643-56.
14. Goicoechea S, Arneman D, Disanza A, Garcia-mata R, Scita G, Otey CA. Palladin binds to Eps8 and enhances the formation of dorsal ruffles and podosomes in vascular smooth muscle cells. J Cell Sci. 2006;119(Pt 16):3316-24.
15. Goicoechea SM, Bednarski B, García-mata R, Prentice-dunn H, Kim HJ, Otey CA. Palladin contributes to invasive motility in human breast cancer cells. Oncogene. 2009;28(4):587-98.
16. Goicoechea SM, Bednarski B, Stack C, et al. Isoform-specific upregulation of palladin in human and murine pancreas tumors. PLoS ONE. 2010;5(4):e10347.
17. Goicoechea SM, García-mata R, Staub J, et al. Palladin promotes invasion of pancreatic cancer cells by enhancing invadopodia formation in cancer-associated fibroblasts. Oncogene. 2014;33(10):1265-73.
18. Von nandelstadh P, Gucciardo E, Lohi J, et al. Actin-associated protein palladin promotes tumor cell invasion by linking extracellular matrix degradation to cell cytoskeleton. Mol Biol Cell. 2014;25(17):2556-70.
19. Asano E, Maeda M, Hasegawa H, et al. Role of palladin phosphorylation by extracellular signal-regulated kinase in cell migration. PLoS ONE. 2011;6(12):e29338.
20. Najm P, El-sibai M. Palladin regulation of the actin structures needed for cancer invasion. Cell Adh Migr. 2014;8(1):29-35.
21. Leong HS, Robertson AE, Stoletov K, et al. Invadopodia Are Required for Cancer Cell Extravasation and Are a Therapeutic Target for Metastasis. Cell Rep. 2014;
22. Cmoch A, Groves P, Pikuła S. Biogenesis of invadopodia and their cellular functions. Postepy Biochem. 2014;60(1):62-8.
23. Saykali BA, El-sibai M. Invadopodia, regulation, and assembly in cancer cell invasion. Cell Commun Adhes. 2014;21(4):207-12.

24. Yang MH, Yu J, Jiang DM, Li WL, Wang S, Ding YQ. microRNA-182 targets special AT-rich sequence-binding protein 2 to promote colorectal cancer proliferation and metastasis. J Transl Med. 2014;12:109.
25. Tay PN, Tan P, Lan Y, et al. Palladin, an actin-associated protein, is required for adherens junction formation and intercellular adhesion in HCT116 colorectal cancer cells. Int J Oncol. 2010;37(4):909-26.

Figure legends

Figure 1. SATB2 expression inhibits invadopodia formation and cancer cell invasion. (A) HCT116 cells that constitutively expressed either FLAG or FLAG-SATB2 were established by retrovirus infection. The cells were fixed with 4% paraformaldehyde and immunostained for F-actin (phalloidin; red) and cortactin (green). Representative micrographs are shown (scale bar = 20 μm) and the graph shows the average percentage of cells with invadopodia (*P<0.05). The arrows indicate the invadopodia concentrations. (B) HCT116 cells were seeded on fluorescein isothiocyanate (FITC)–gelatin (green), fixed with 4% paraformaldehyde and immunostained for cortactin (red). Representative micrographs are shown (scale bar = 20 μm). (C) FLAG or FLAG-SATB2 HCT116 cells were subjected to an invasion assay. Representative images of invaded cells are shown, and the graph indicates the average number of invaded cells per field (*P<0.05).

Figure 2. SATB2 expression inhibits palladin expression. (A) HCT116 cells constitutively expressing GFP (GFP) or GFP-tagged SATB2 (GFP-SATB2) were generated by retroviral infection. The expression of GFP or GFP-SATB2 proteins in each cell line was examined by immunoblotting using anti-GFP and anti-SATB2 antibodies. An arrow indicates the endogenous SATB2. (B) The level of palladin mRNA in GFP- and GFP-SATB2 cells was determined by qRT-PCR (C) Palladin expression in either GFP or GFP-SATB2 expressing cells was determined by immunoblotting. The arrows indicates the 200, 140, 115, 90 and 50 kDa palladin isoforms.

Figure 3. Palladin depletion reduces cancer cell migration and invasion. (A) Palladin expression was detected in seven colorectal cancer cell lines by immunoblotting. (B) HCT116 cells constitutively expressing shCtrl, shPALLD #1 and shPALLD #2 were generated by retroviral infection. The palladin expression was detected in these cell

lines by immunoblotting. (C) Confluent monolayers of shCtrl, shPALLD #1 or shPALLD #2 HCT116 cells were scratched, and cell migration was examined every 12 h. Representative images of migrated cells are shown, and the graph shows the average migrated distance at the indicated time points (*P<0.05). (D) ShCtrl, shPALLD #1 or shPALLD #2 HCT116 cells were subjected to the migration assay. Representative images of migrated cells are shown, and the graph indicates the average number of migrated cells per field (*P<0.05). (E) ShCtrl, shPALLD #1 or shPALLD #2 HCT116 cells were subjected to an invasion assay. Representative images of invaded cells are shown, and the graph indicates the average number of invaded cells per field (*P<0.05).

Figure 4. Palladin depletion inhibits invadopodia formation. (A) HCT116 cells that constitutively expressed shCtrl, shPALLD #1 or shPALLD #2 were fixed with 4% paraformaldehyde and immunostained for F-actin (phalloidin; red) and cortactin (green). Representative micrographs are shown (scale bar = 20 μm) and the graph shows the average percentage of cells with invadopodia (*P<0.05). The arrows indicate the invadopodia concentrations. (B) HCT116 cells were fixed with 4% paraformaldehyde and immunostained for cortactin (green) and palladin (red). Representative micrographs are shown (scale bar = 20 μm).

Figure 5. Rescue of palladin restores invadopodia formation. (A) HCT116 constitutively expressing shCtrl, shPALLD #2/GFP and shPALLD #2/GFP PALLD (Res) were generated by retroviral infection. The endogenous and exogenous palladin expression was detected in these cell lines by immunoblotting using anti-palladin and anti-GFP. An arrow indicates exogenous palladin level. (B) HCT116 cells that constitutively expressed shPALLD #2/GFP and shPALLD #2/GFP PALLD (Res) were fixed with 4% paraformaldehyde and immunostained for GFP (green) and cortactin (red). Representative micrographs are shown (scale bar = 20 μm). The graph indicates the average percentage of cells with invadopodia in the cells (*P<0.05).

Figure 6. Palladin expression restores invadopodia formation in SATB2-expressing cells. (A) HCT116 cells constitutively expressing FLAG, FLAG-SATB2/GFP and FLAG-SATB2/GFP-palladin were generated by retroviral infection. Endogenous and exogenous palladin expression were detected by immunoblotting using anti-palladin and confirmed by anti-GFP. An arrow indicates the exogenous palladin expression (B) HCT116 cells that constitutively expressed FLAG-SATB2/GFP were fixed with 4% paraformaldehyde and immunostained for GFP (green) and cortactin (red).

Representative micrographs are shown (scale bar = 20 μm) (C) HCT116 cells that constitutively expressed FLAG-SATB2/GFP-palladin (wt) were fixed with 4% paraformaldehyde and immunostained for GFP (green) and cortactin (red). Representative micrographs are shown (scale bar = 20 μm). The graph indicates the average percentage of cells with invadopodia in FLAG-SATB2/GFP and FLAG-SATB2/GFP-palladin cells (*P<0.05).

Figure 1

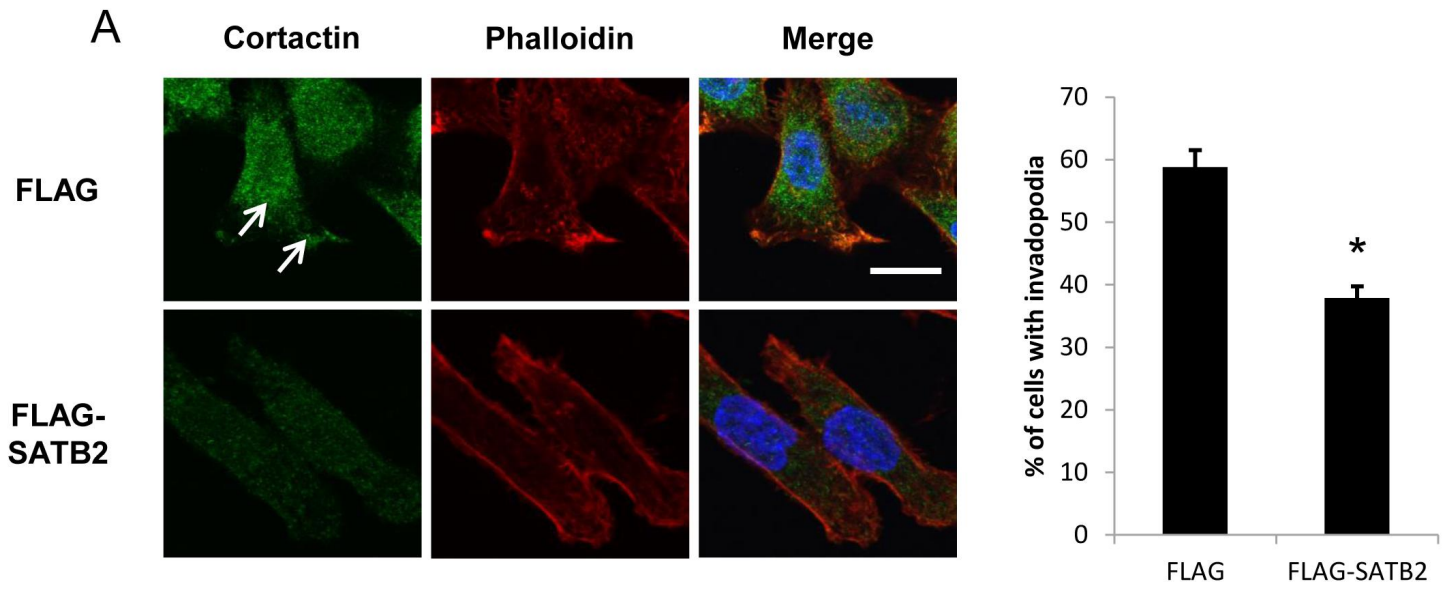
A
Cortactin
Phalloidin
Merge
FLAG
FLAG-SATB2
% of cells with invadopodia
70
60
50
40
30
20
10
0
*
FLAG
FLAG-SATB2

Figure 2

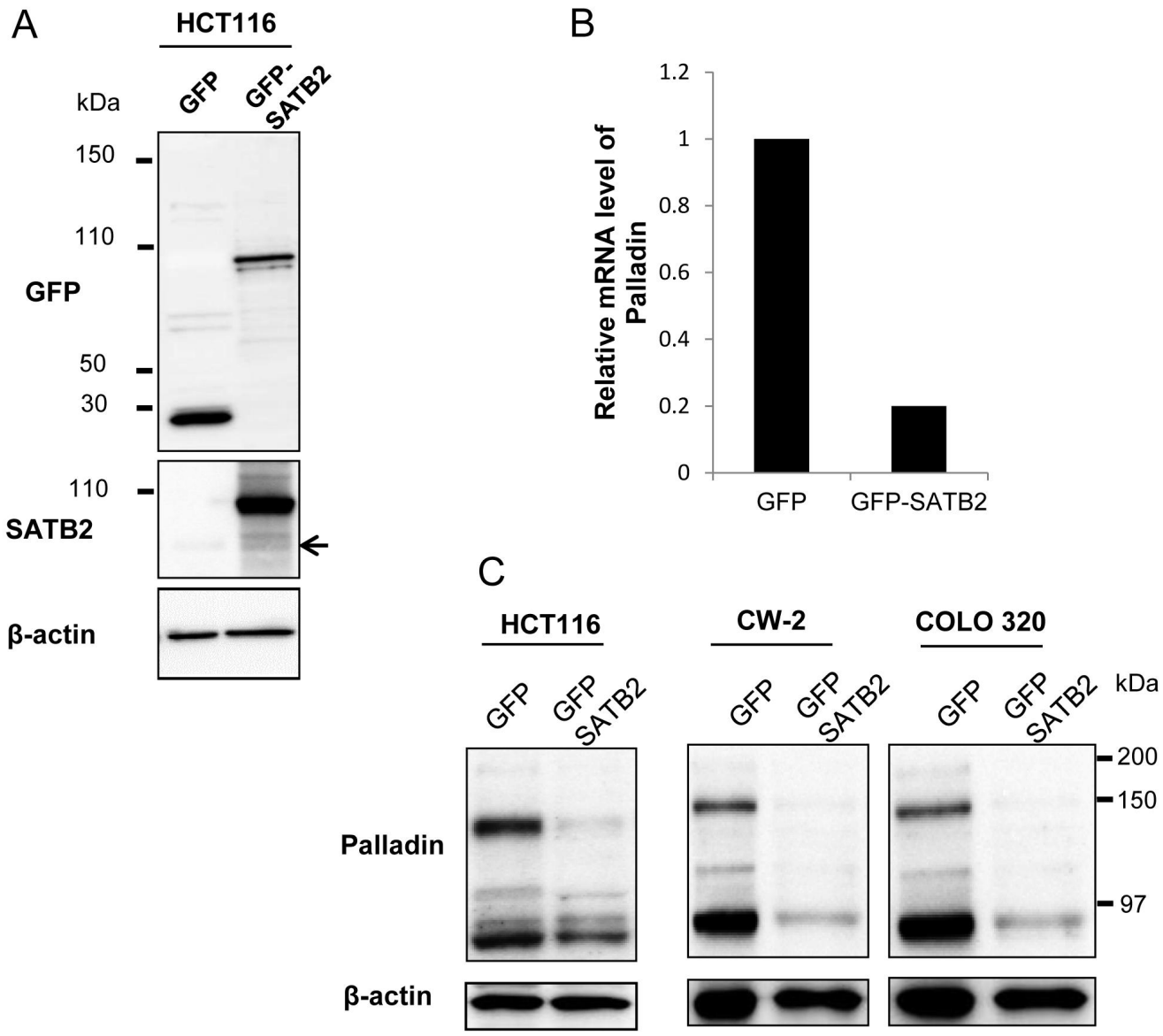
A
HCT116
kDa
GFP
GFP-SATB2
150
110
GFP
50
30
110
SATB2
β-actin
B
Relative mRNA level of Palladin
1.2
1
0.8
0.6
0.4
0.2
0
GFP
GFP-SATB2
C
HCT116
CW-2
COLO 320
GFP
GFP SATB2
kDa
200
150
97
Palladin
β-actin

Figure 3

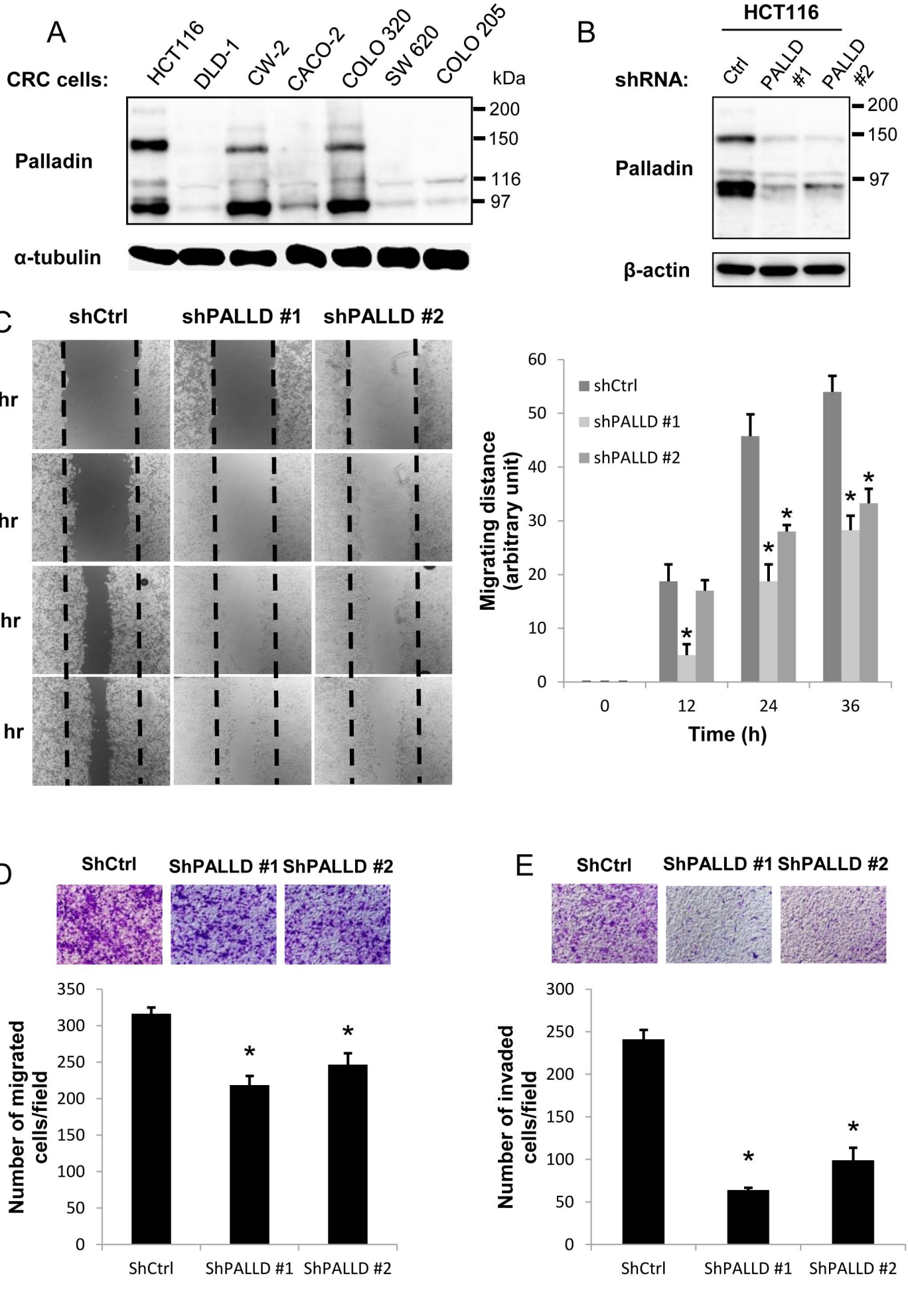
A
CRC cells:
HCT116
DLD-1
CW-2
CACO-2
COLO 320
SW 620
COLO 205
kDa
Palladin
200
150
116
97
α-tubulin
B
HCT116
shRNA:
Ctrl
PALLD #1
PALLD #2
Palladin
200
150
97
β-actin
C
shCtrl
shPALLD #1
shPALLD #2
0 hr
12 hr
24 hr
36 hr
Migrating distance (arbitrary unit)
shCtrl
shPALLD #1
shPALLD #2
Time (h)
D
ShCtrl
ShPALLD #1
ShPALLD #2
Number of migrated cells/field
E
ShCtrl
ShPALLD #1
ShPALLD #2
Number of invaded cells/field

Figure 4

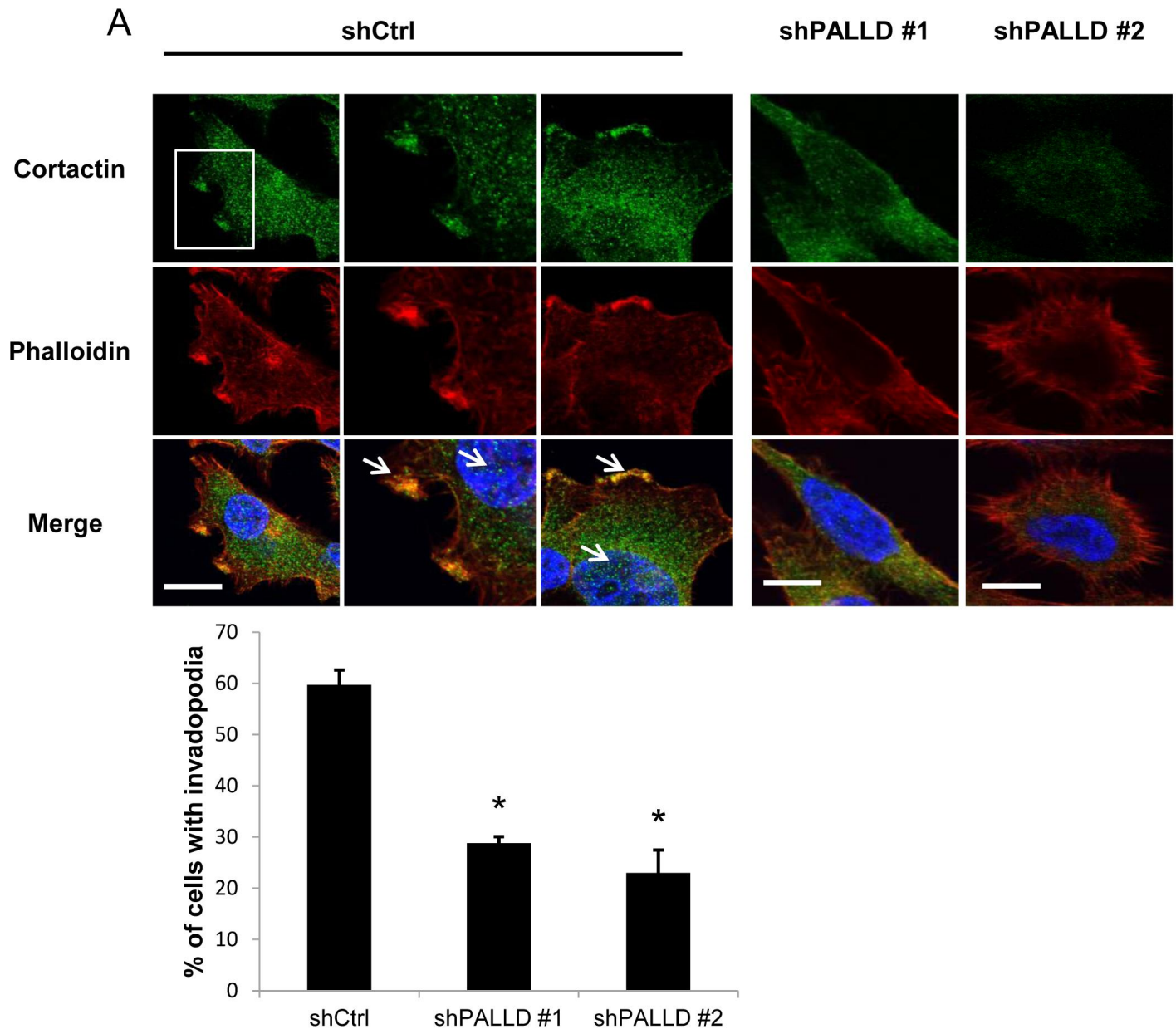
A
shCtrl
shPALLD #1
shPALLD #2
Cortactin
Phalloidin
Merge
% of cells with invadopodia
70
60
50
40
30
20
10
0
*
*
shCtrl
shPALLD #1
shPALLD #2

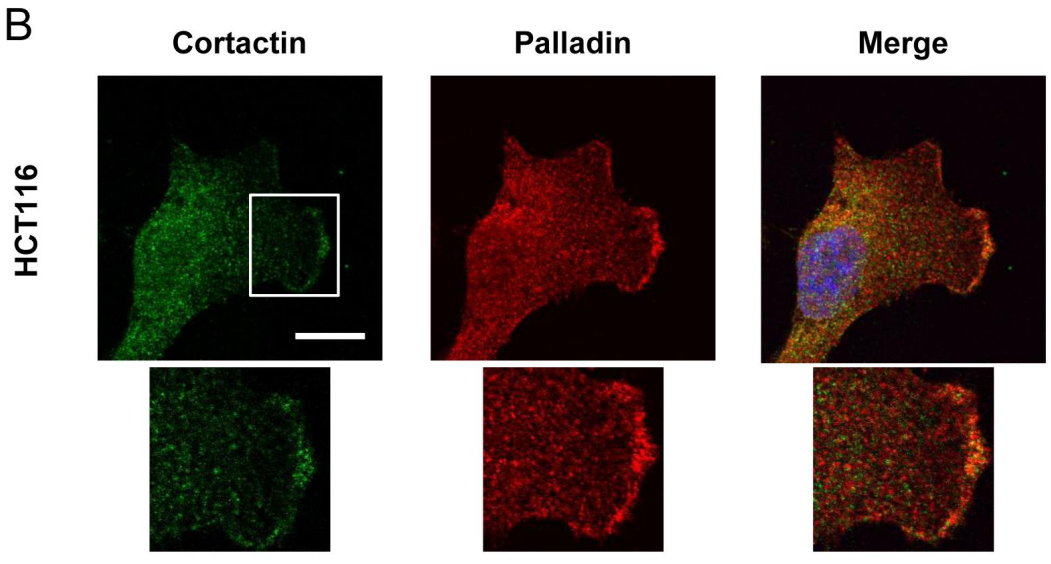
B
Cortactin
Palladin
Merge
HCT116

Figure 5

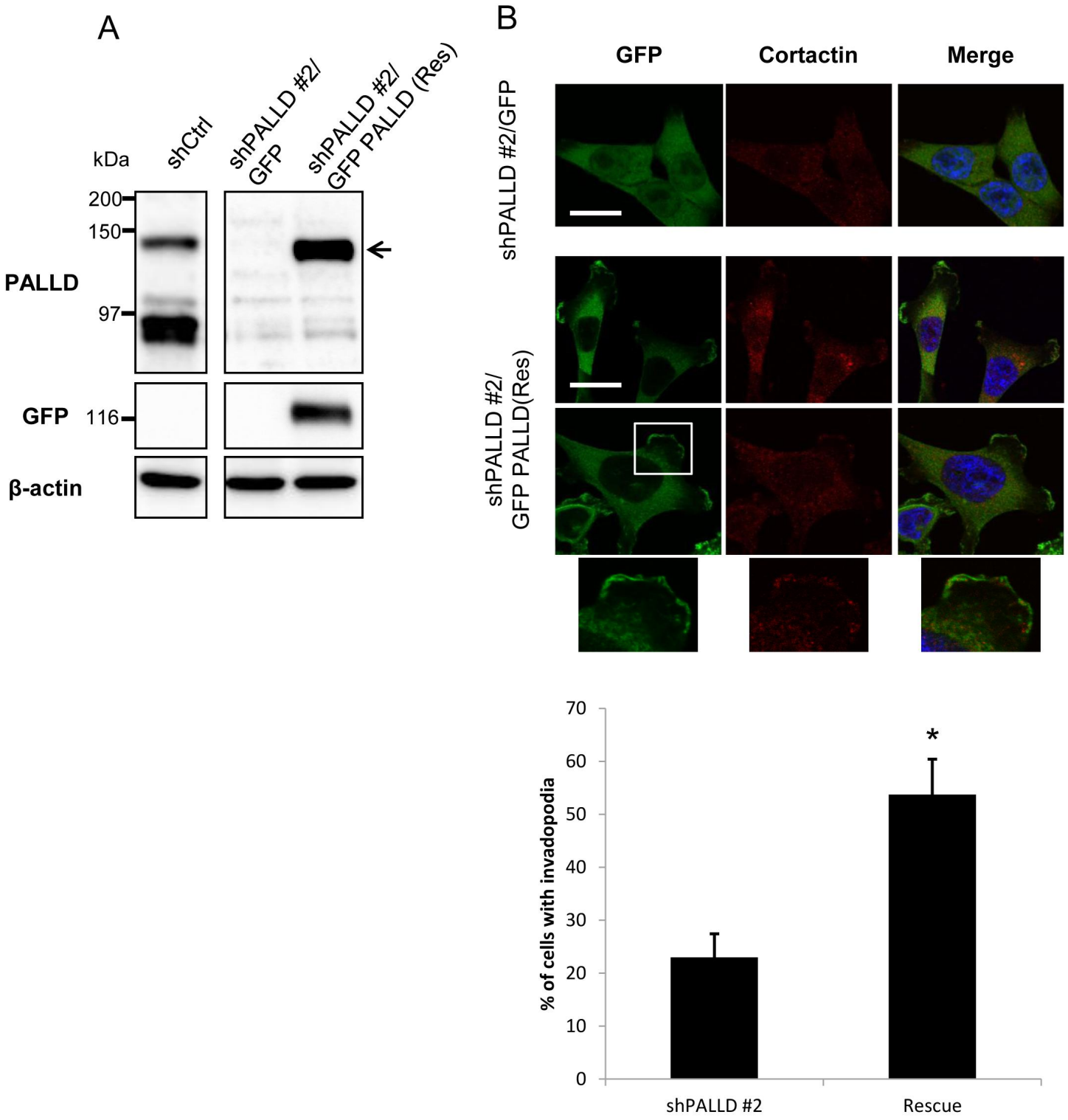
A
shCtrl
shPALLD #2/ GFP
shPALLD #2/ GFP PALLD (Res)
kDa
200
150
PALLD
97
GFP
116
β-actin
B
GFP
Cortactin
Merge
shPALLD #2/GFP
shPALLD #2/ GFP PALLD(Res)
% of cells with invadopodia
70
60
50
40
30
20
10
0
*
shPALLD #2
Rescue

Figure 6

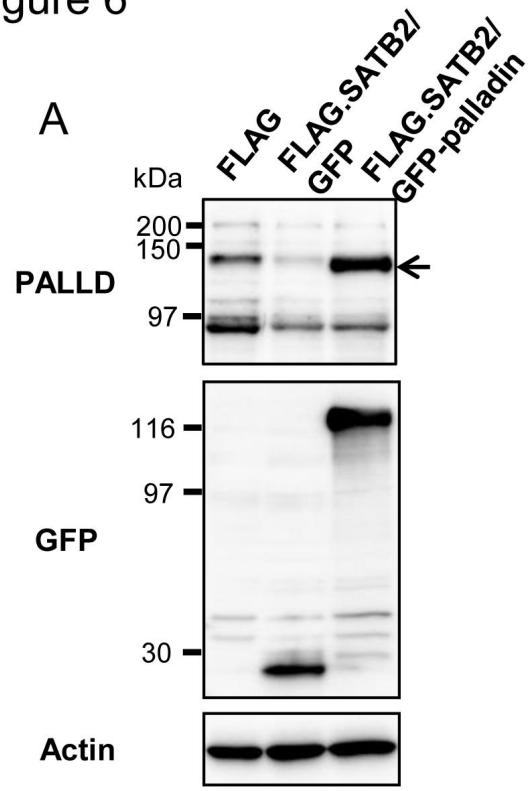
A
FLAG
FLAG.SATB2/ GFP
FLAG.SATB2/ GFP-palladin
kDa
200
150
PALLD
97
116
97
GFP
30
Actin

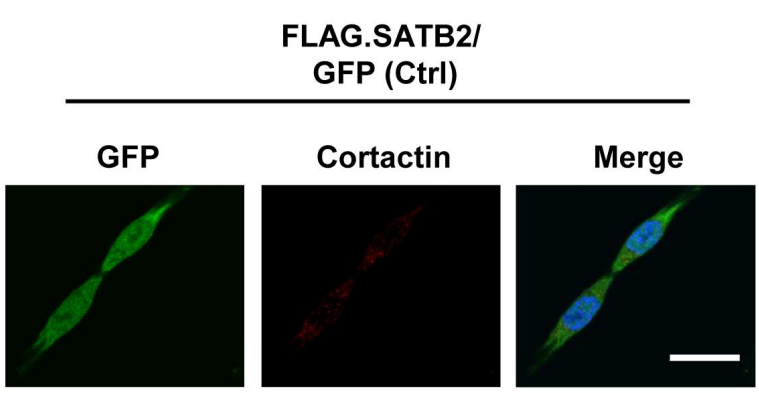
B
FLAG.SATB2/ GFP (Ctrl)
GFP
Cortactin
Merge

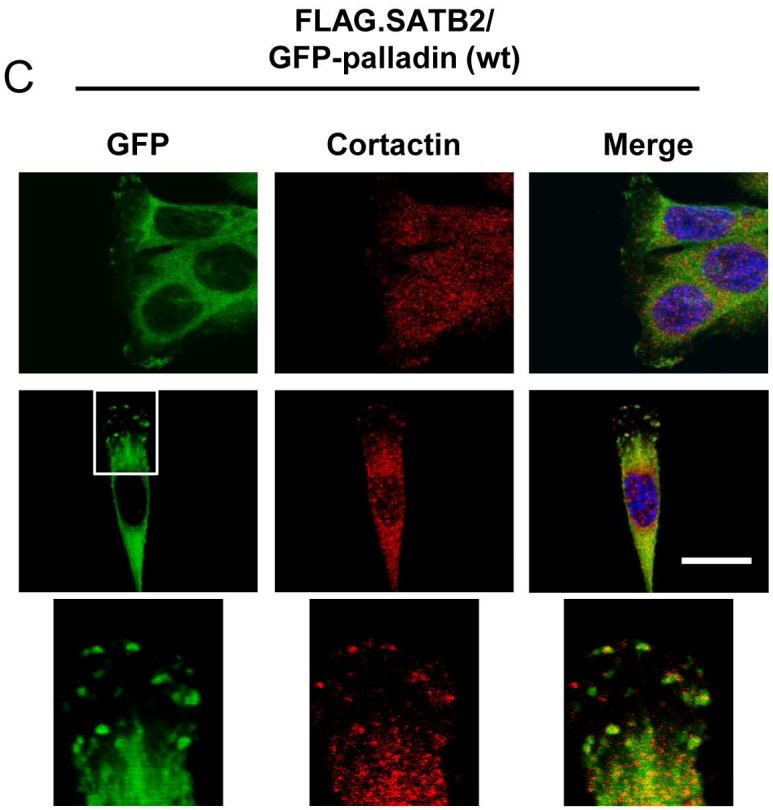
C
FLAG.SATB2/ GFP-palladin (wt)
GFP
Cortactin
Merge

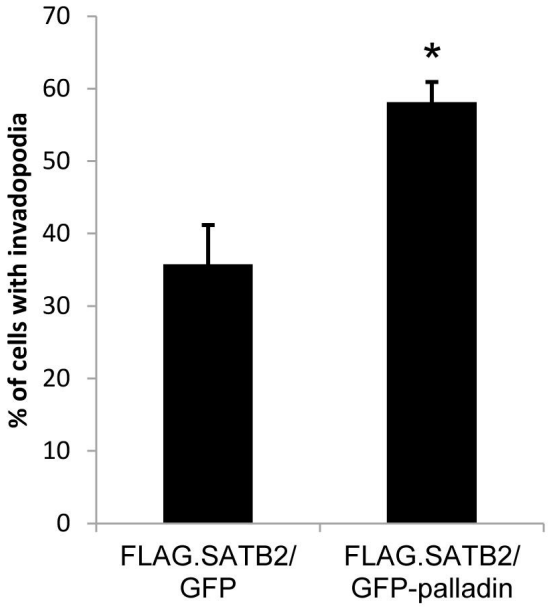
70
60
50
40
30
20
10
0
% of cells with invadopodia
*
FLAG.SATB2/ GFP
FLAG.SATB2/ GFP-palladin